Application of industrial amylolytic yeast strains for the production of bioethanol from broken rice

Marthinus W. Myburgh[a], Rosemary A. Cripwell[a], Lorenzo Favaro[b]*, Willem H. van Zyl[a]

[a]*Department of Microbiology, Stellenbosch University, Private Bag X1, Matieland 7602, South Africa*

18182267@sun.ac.za; rosecripwell@sun.ac.za; whvz@sun.ac.za

[b]*Department of Agronomy Food Natural resources Animals and Environment (DAFNAE), Padova University, Agripolis, Viale dell'Università 16, 35020 Legnaro, Padova, Italy*

*Corresponding author: **Lorenzo Favaro, PhD**

Department of Agronomy Food Natural resources Animals and Environment (DAFNAE)

Agripolis - University of Padova

Viale dell'Università, 16

35020 Legnaro, PADOVA, ITALY

Tel. 049-8272800 (926)

Fax 049-8272929

e-mail: lorenzo.favaro@unipd.it

Abstract

Amylolytic *Saccharomyces cerevisiae* derivatives of Ethanol Red™ Version 1 (ER T12) and M2n (M2n T1) were assessed through enzyme assays, hydrolysis trials, electron microscopy and fermentation studies using broken rice. The heterologous enzymes hydrolysed broken rice at a similar rate compared to commercial granular starch-hydrolysing enzyme cocktail. During the fermentation of 20% dw/v broken rice, the amylolytic strains converted rice starch to ethanol in a single step and yielded high ethanol titers. The best-performing strain (ER T12) produced 93% of the theoretical ethanol yield after 96 h of consolidated bioprocessing (CBP) fermentation at 32°C. Furthermore, the addition of commercial enzyme cocktail (10% of the recommended dosage) in combination with ER T12 did not significantly improve the maximum ethanol concentration, confirming the superior ability of ER T12 to hydrolyse raw starch. The ER T12 strain was therefore identified as an ideal candidate for the CBP of starch-rich waste streams.

Keywords: raw starch; broken rice; bioethanol production; consolidated bioprocessing; amylolytic industrial yeast.

1. Introduction

The microbial conversion of biomass to value-added products is an attractive alternative to fossil fuels and continues to gain interest, especially with the rise in global environmental awareness. Although second-generation biofuel production from lignocellulosic biomass has made some progress in recent years with four commercial cellulosic ethanol plants in the U.S. (Renewable Fuels Association, 2017; Favaro et al., 2019), starch-based feedstocks are still predominantly used in the bioethanol industry. Corn is the preferred substrate for large-scale bioethanol production (Niphadkar et al., 2018) due to the ease of long-term storage, nontoxicity and high reactivity of corn starch (Zabed et al., 2017). Indeed, the production of biofuels from corn starch is considered a mature technology with 15.8 billion gallons of fuel ethanol produced in 2017 in the U.S. (Renewable Fuels Association, 2017). However, the corn-based feedstock represents one of the main costs involved in the production of bio-based ethanol (Favaro et al., 2013; Yu et al., 2019). Thus, there is a need for alternative low-cost feedstocks (Niphadkar et al., 2018). Cheap and abundant starchy by-products from industries, such as food and agricultural processing, are good candidates in this regard (Atitallah et al., 2019; Nizami et al., 2017; Ntaikou et al, 2018).

According to the Food and Agriculture Organization (FAO) of the United Nations, global paddy production reached 770 million tons in 2018, making rice production one of the largest grain industries in the world. The processing of rice results in a range of by-products, including rice bran, rice husk as well as unripe, discoloured and broken rice. The starch content of these by-products typically ranges from 7-85% of the dry weight, with discoloured and broken rice having the highest starch concentration (Favaro et al., 2017). Given its high starch content and

annual abundance (45 million tons in 2014), broken rice has become a good alternative feedstock for starch-to-ethanol technologies (Chu-Ky et al., 2016; Gronchi et al., 2019).

Irrespective of the feedstock, there are other substantial costs linked to current starch-to-ethanol production processes. These are predominantly associated with the conventional energy-intensive gelatinization step, or the addition of exogenous enzyme cocktails for the liquefaction and saccharification of raw starch (Chandel et al., 2018; Sakwa et al., 2018). It is estimated that the energy requirement for conventional gelatinization accounts for 10-20% of the fuel value of the ethanol in a typical refinery (Meredith, 2003). Moreover, the cost of enzymes is equivalent to 8% of the total processing cost (Favaro et al., 2010; Görgens et al., 2015). The production of ethanol from starch can therefore benefit from the combination of all these steps into a single process called consolidated bioprocessing (CBP). In such a process genetically engineered ethanologenic yeast strains, like amylolytic *Saccharomyces cerevisiae* strains, are required to produce raw starch-degrading enzymes that enable the yeast to simultaneously hydrolyse the starch and ferment the resulting sugars to ethanol (Chandel et al., 2018; Cripwell et al., 2019a).

A number of *S. cerevisiae* strains with raw starch CBP capabilities have been developed in the past with varying degrees of success (Favaro et al., 2015; Sakwa et al., 2018; Viktor et al., 2013). Favaro et al. (2017) evaluated two recombinant amylolytic *S. cerevisiae* strains, namely MEL2[TLG1-SFA1] and M2n[TLG1-SFA1], in terms of their ability to ferment a variety of rice-waste products, including broken rice, in a CBP process. The strains were capable of CBP, producing approximately 70 g/L of ethanol from broken rice after 144 h of fermentation. However, if broken rice is to be used for bioethanol production on a commercial scale, higher ethanol concentrations (10-12% v/v or 70-100 g/L) are required in shorter fermentation times (50-70 h) (Mathew et al., 2015). This could potentially be attained through the use of improved

amylolytic yeast strains that show better enzymatic hydrolysis of raw starch and produce higher ethanol yields.

Recently, amylolytic strains of *S. cerevisiae* Ethanol Red™ Version 1 (referred to as ER) and M2n were developed by Cripwell et al. (2019b) to simultaneously secrete an α-amylase and glucoamylase originating from *Talaromyces emersonii*. The industrial strains, named ER T12 and M2n T1, showed superior fermenting capabilities in the CBP of raw corn starch at high substrate loadings (20% dw/v) and displayed exceptional volumetric amylase activity. Further investigation and assessment of these strains is required to establish their fermentation capabilities on different and more industrially relevant starch-based substrates.

In this study, the two recombinant amylolytic *S. cerevisiae* strains, ER T12 and M2n T1, were evaluated for their ability to simultaneously hydrolyse raw broken rice and produce ethanol. The supernatants from ER T12 and M2n T1, containing recombinant α-amylase and glucoamylase, were first evaluated in terms of the saccharification of broken rice. Subsequently, different fermentation configurations were compared and the additive effect of an exogenous granular starch hydrolysing enzyme (GSHE) cocktail on ethanol production was determined. Finally, the fermentation of broken rice to ethanol under more industrially relevant conditions (i.e. no added nutrients or media components) was validated at different temperatures.

2. Materials and methods

2.1 Strains, media and cultivation

Four industrial *S. cerevisiae* strains were used during the current study (Table 1). This included two parental (non-recombinant) strains, M2n and ER, and their respective recombinant strains, M2n T1 and ER T12 (Cripwell et al., 2019b). Yeast strains were maintained on YPD

agar (10 g/L yeast extract, 20 g/L peptone, 20 g/L glucose and 20 g/L agar) at 30°C and were routinely cultured in YPD broth. All media components and reagents were supplied by Sigma-Aldrich (Steinheim, Germany) unless stated otherwise.

Table 1:

2.2 Chemical analysis of broken rice

The broken rice was obtained from La Pila (Isola della Scala, Italy). The rice by-product was dried in a forced-air oven at 55°C, milled and then sieved through a 1.25 mm screen. The starch, cellulose, hemicellulose, lignin, ash and protein content was determined according to international standard methods (AOAC, 2000).

2.3 Enzyme activity assays

Volumetric assays were conducted using reducing sugar assays with dinitrosalicilic acid (DNS) (Miller, 1959). Briefly, all strains were inoculated at an absorbance value of 0.1 (600 nm) in 125 mL Erlenmeyer flasks containing 25 mL YPD broth. Volumetric enzyme activity was determined using 0.1% soluble potato starch (Sigma-Aldrich) dissolved in 0.05 M citrate buffer (pH 5) as substrate. Assays were conducted at 50°C for 10 min and absorbance readings were taken at 540 nm using a TECAN Spark 20M microplate spectrophotometer (TECAN, Salzburg, Austria). All activities are reported as units per millilitre (U/ml), where one unit is defined as the amount of enzyme required to release 1 µmol of glucose per minute. Protein concentrations were determined in parallel to volumetric assays using Bradford reagent (Sigma-Aldrich) according to the manufacturer's instructions.

The thermal stability of the *T. emersonii* crude α-amylase and glucoamylase enzymes was determined using supernatant from yeast cultures (grown in YPD broth at 30°C for 72 h)

incubated at 30 and 37°C for 168 h. Samples of the supernatant were taken at specific intervals and the residual enzymatic activity was determined.

2.4 Hydrolysis trials on raw broken rice

The ability of the crude amylases to hydrolyse broken rice to glucose was evaluated using hydrolysis trials at 30°C in a rotating hybridisation chamber. Supernatant from the recombinant strains, grown in YPD broth for 72 h at 30°C, was collected and added to 10 mL tubes (5 mL working volume) containing 2% dw/v broken rice and 0.02% w/v sodium-azide (to prevent microbial growth). Samples of the supernatant were removed at regular intervals and analysed with an adapted DNS protocol and high-pressure liquid chromatography (HPLC) as described in *2.7 Analytical methods and calculations.*

A scaled up cell-free hydrolysis configuration was used to compare the recombinant enzymes produced by ER T12 to that of the STARGEN^{TM} 002 commercial enzyme cocktail. STARGEN^{TM} 002 (referred to as GSHE in this study) from DuPont Industrial Biosciences (Palo Alto, California, USA) was used as a percentage of the manufacturers recommended dosage (DuPont, 2012). Supernatant from the parental *S. cerevisiae* ER and the engineered ER T12 strains was added to separate 125 mL serum bottles containing 20% dw/v broken rice substrate (100 mL working volume) and 0.02% w/v sodium-azide. Selected GSHE loadings (200, 100 and 50% of the recommended enzyme dosage) were added to bottles containing supernatant from the parental *S. cerevisiae* ER strain. Samples were taken at regular intervals and analysed using HPLC analysis. All experiments were performed in triplicate.

158 *2.5 Scanning electron microscopy*

159 Scanning electron microscopy (SEM) was employed to visualise hydrolysis of the broken
160 rice. Samples from the scaled up hydrolysis configurations were placed on 0.22 µm filters,
161 washed with 70% ethanol and dehydrated with 100% ethanol. The samples were mounted onto
162 standard 12 mm SEM aluminium pin stubs and gold coated (8 nm) with a Leica EM ACE200
163 sputter-coater (Leica Microsystems, Germany) to enhance conductivity. SEM imaging was done
164 using a Zeiss Merlin Field Emission SEM (Carl Zeiss Microscopy, Germany) operated at 2-3 kV
165 accelerating voltage, 89-100 pA beam current and using InLens Secondary Electron (SE) and
166 SE2 detection.

167

168 *2.6 Fermentations*

169 Three different fermentation configurations were performed, i.e. simultaneous
170 saccharification and fermentation (SSF using exogenous GSHE for starch hydrolysis), CBP
171 supplemented with GSHE (recombinant yeast strains with exogenous GSHE addition) and
172 conventional CBP (only recombinant yeast strains). Small-scale fermentations were conducted in
173 120 mL glass serum bottles as described by Viktor et al. (2013), with rubber stoppers ensuring
174 oxygen-limited conditions. The serum bottles contained 70 mL concentrated YPD (5 g/L
175 glucose), 20% dw/v broken rice and a 10% v/v inoculum from 72 h aerobic pre-cultures. This
176 inoculum size was specifically chosen to compare the recombinants' fermenting abilities to those
177 of other CBP amylolytic yeast strains (Viktor et al., 2013; Favaro et al., 2015, 2017; Yamada et
178 al., 2010).The wet cell weight of the 10% v/v inoculum was determined according to Viktor et al.
179 (2013). Ampicillin (100 µg/mL) and streptomycin (50 µg/mL) were added to limit bacterial
180 growth.

Commercial GSHE was added at 100% of the recommended dosage for the parental *S. cerevisiae* ER and M2n strains during SSF, at 10% for the recombinant *S. cerevisiae* ER T12 and M2n T1 strains during supplemented CBP or at 0% (no GSHE added) for *S. cerevisiae* ER T12 and M2n T1 strains during conventional CBP fermentations. The serum bottles were incubated at 32°C on a magnetic stirrer (IKA, Staufen, Germany) set at 360 rpm. Daily samples were collected up to 168 h for HPLC quantification of ethanol, glucose, glycerol, acetic acid and maltose concentrations.

The ability of *S. cerevisiae* ER T12 to utilise broken rice without any media supplementation was evaluated with a conventional CBP configuration using only 70 mL sterilised reverse osmosis (RO) water and 20% dw/v broken rice. To test the effect of nitrogen supplementation, CBP fermentations were also performed using 70 mL RO water, 20% dw/v broken rice and 16 mM urea (Devantier et al., 2005). These CBP fermentations (using RO water) were compared to CBP fermentations with concentrated YPD at 30 and 37°C on a magnetic stirrer set at 360 rpm. All fermentation experiments were performed in triplicate.

2.7 Analytical methods and calculations

Prior to HPLC analyses, liquid fractions from collected samples were diluted and filtered using 0.22 µmm nylon syringe filters. Chromatography was performed using a Shimadzu Nexera HPLC system equipped with a RID-10A refractive index detector (Shimadzu, Kyoto, Japan). Chromatographic separations were performed using a Phenomenex Rezex ROA-Organic Acid H^+ (8%) column (300 mm×7.8 mm) with the column temperature kept at 80°C. The analysis was performed at a flow rate of 0.6 mL/min using isocratic elution and 5 mM H_2SO_4 as a mobile phase. Maltose, glucose, acetic acid, ethanol and glycerol were identified by correlating retention times and their concentrations were calculated using standard calibration curves from external

standards. Theoretical CO_2 yields were calculated based on ethanol production, assuming that ethanol and CO_2 are produced in equimolar fractions. The percentage of available carbon converted into the various fermentation products (referred to as estimated carbon conversion) was determined on a mole carbon basis (Cripwell et al., 2019b). Ethanol yield ($Y_{E/S}$) is reported as a percentage of the theoretical maximum (0.51 g/L per glucose equivalent) based on the total available glucose equivalents.

The degree of saccharification (DS) of the broken rice represents the amount of soluble sugars released after hydrolysis and was calculated as the sum of glucose and maltose concentrations divided by the available starch. A conversion factor of 0.9 and 0.95 was included to reflect the addition of a water molecule during hydrolysis (Cripwell et al., 2015).

$$DS = \frac{[glucose\ g/L \times 0{,}9] + [maltose\ g/L \times 0{,}95]}{[available\ starch\ g/L]}$$

3. Results and discussion

3.1 Substrate composition, activity assays and enzyme stability of the recombinant amylases

Chemical analysis of the broken rice showed a starch content of 83.8% of the substrate dry matter, as well as low levels of cellulose, hemicellulose and ash (no lignin was detected) (Supplementary material). These secondary compounds are associated with rice milling by-products at different concentrations, e.g. the cellulose content can range from 0.1% in discoloured rice to 4.6% in rice bran (Favaro et al., 2017). They may also have an inhibitory effect on starch hydrolysis by rendering starch granules less accessible to enzymes or mediating direct binding of amylases, as is the case with cellulose (Dhital et al., 2015). Low levels of cellulose, hemicellulose and lignin are thus preferred in starch-based industrial substrates. A substantial amount of protein was detected in the substrate (8.5%), which agreed with other

findings that showed proteins loosely associating with cereal starch granules (Bertoft, 2017; Gohel and Duan, 2012). However, this is lower than reported for other complex substrates, such as wheat bran that can contain up to 18% protein (Cripwell et al., 2015; Favaro et al., 2012a; Theander et al., 1995). The level of protein in the broken rice is noteworthy as it may serve as a nitrogen source for yeast during fermentation (Bothast and Schlicher, 2005). The high starch content, low levels of secondary compounds and presence of proteins in the substrate support the suitability of broken rice as a starch-based feedstock for bioethanol production via CBP.

The recombinant *S. cerevisiae* ER T12 and M2n T1 strains showed high levels of volumetric amylase activity with a maximum of 9.83 and 4.47 U/mL, respectively, after 72 h aerobic cultivation in YPD (Fig. 1A). This is in agreement with higher levels of enzymatic activity previously reported for *S. cerevisiae* ER T12 than for M2n T1 (Cripwell et al., 2019b). Although *S. cerevisiae* also secretes native proteins, the increase in amylase activity showed a positive correlation with extracellular protein levels ($r = 0.85$, $p < 0.01$), with 279 and 213 µg/mL protein being produced after 72 h by ER T12 and M2n T1, respectively. Furthermore, it is important that the recombinant enzymes remain stable at fermentation temperatures over long incubation times to ensure efficient starch hydrolysis (Cripwell et al., 2019a; Favaro et al., 2012b; Görgens et al., 2015). The crude enzymes secreted by both recombinant strains exhibited high stability at 30 and 37°C, with no loss in amylolytic activity over 168 h of incubation (Supplementary material).

Fig. 1.

3.2 Enzymatic hydrolysis of raw broken rice

The crude enzymes secreted by *S. cerevisiae* ER T12 and M2n T1 were assessed for the saccharification of broken rice in trials using a 2% dw/v substrate loading (Fig. 1B). The novel

amylase combination secreted by the industrial strains was effective in hydrolysing the starch component of broken rice, with an increase in total reducing ends over time observed for the supernatant from both the ER T12 and M2n T1 strains (Fig. 1B). Supernatant from the ER T12 strain generally released more reducing sugars from broken rice and at an earlier time point than M2n T1. Final DS values of 30 and 17% were reached after 96 h for the ER T12 and M2n T1 strains, respectively, further supporting the higher saccharification capability of crude enzymes from *S. cerevisiae* ER T12.

3.3 Scaled up hydrolysis with ER T12 versus a GSHE cocktail

To assess the ability of the recombinant enzymes to hydrolyse rice-starch at higher substrate loadings, the supernatant of *S. cerevisiae* ER T12 was compared to different dosages of a GSHE cocktail on 20% dw/v raw broken rice (representing a 10-fold increase in substrate loading). The selected STARGEN^{TM} 002 GSHE cocktail is considered by industry as one of the most efficient amylase cocktails for raw starch hydrolysis (Gronchi et al., 2019) and is recommended to be used at a dosage of 28.3 µl per 100 mL (1 g/kg of substrate) (DuPont, 2012).

When the three GSHE loadings (50, 100 and 200% of the recommended dosage) were combined with supernatant from the parental ER strain, a steady increase in glucose levels was observed over time (Fig. 2A). Noteworthy, a similar increase was detected for samples incubated with crude enzymes from the recombinant ER T12 strain. The latter compared well to the parental strain supplemented with a 100% GSHE loading at 72 h, but the free glucose concentration at 168 h was more similar to hydrolysis with a 50% GSHE loading. The maltose concentrations fluctuated over the first 120 h, and an increased maltose concentration, that reflected the increased enzyme loadings, was observed after 144 h (Fig. 2B). This may suggest

possible product (glucose) inhibition of the glucoamylase (from both GSHE and recombinant enzymes) after the prolonged hydrolysis (Wang et al., 2006).

The DS by the crude recombinant enzymes was comparable to that achieved by a 100% GSHE loading after 72 h (Fig. 2C). After 168 h of enzymatic hydrolysis, the DS values of broken rice were still increasing thus indicating that amylase activity was sufficient at a substrate loading of 20% dw/v with continued and efficient hydrolysis over a prolonged period of time. This is in agreement with previous studies reporting amylases with high enzyme stability over time at different fermentation temperatures (Liao et al., 2012; Görgens et al., 2015; Sakwa et al., 2018).

To our knowledge, this is the first report describing such a high saccharification by crude enzymes produced by a recombinant *S. cerevisiae* strain on a complex starchy substrate, comparable to that of a specifically developed commercial product, i.e. STARGEN™ 002.

Fig.2

3.4 Visualization of starch hydrolysis through SEM

Scanning electron microscopy was used to visually evaluate rice-starch granules for signs of degradation and differences in modes of action by crude recombinant enzymes from ER T12 and/or the GSHE cocktail (Supplementary material). SEM analysis confirmed the size (2-10 µm) and sharp-edged morphology characteristic of rice-starch granules (Blazek and Gilbert, 2010). Spherical superstructures, known as compound granules, were also noted as the starch granules associate with each other. Unlike the simple starch granules in corn, compound granules are formed in rice through the assembly of seven or more starch granules (Matsushima et al., 2015). Although the smaller starch granules in the compound granules remain unfused, the structures

297 are supported by other polymers (white arrows in Supplementary material), assumed to be
298 fractions of cellulose, hemicellulose and lignin.
299 After 72 h of hydrolysis, the compound granules were absent and only individual granules
300 were observed, with supporting polymers still present albeit at lower frequencies (white arrow
301 Supplementary material). The separation of the compound granules is attributed to physical
302 agitation during the experiment and not hydrolytic activity by amylases on the supporting
303 polymers. However, the association of these polymers with starch granules and the observation
304 that they support compound granules may restrict the accessibility of starch granules to enzymes,
305 thereby decreasing starch hydrolysis and subsequently ethanol production (Sindhu et al., 2016).
306 SEM confirmed the physical degradation of starch granules for all the samples incubated with
307 ER T12 supernatant or parental ER supernatant supplemented with GSHE (50 or 200%
308 loadings). The enzymes hydrolysed the starch granules through different modes of centripetal
309 action (from surface to centre), namely small pit formation and larger pore formation. Pit
310 formation, also referred to as “Swiss cheese hydrolysis”, describes the deep small holes forming
311 on the surface of the starch granule (Sujka and Jamroz, 2007). In contrast to small pit formation,
312 single, large and seemingly deeper pores were also observed in treated starch granules.
313 Centripetal hydrolysis and pit formation in A-type cereal starches, such as rice, are key to the
314 diffusion of enzymes into the substrate (Blazek and Gilbert, 2010). This may suggest that the
315 hydrolytic enzymes penetrated the granule through pores and pits, which resulted in an endo-
316 erosion, or inside-out hydrolysis of the granule (black arrow in Supplementary material).
317 Centrifugal (only peripheral) hydrolysis was observed in samples incubated with either ER
318 T12 supernatant or ER with GSHE loadings, exposing striations on the surface of the starch
319 granule. This type of granular erosion is typically associated with B-type tuber starches (Blazek

and Gilbert, 2010). These ridges are known as ‘growth rings’ and are the interspersed semi-crystalline and amorphous regions of the starch granule. The semi-crystalline regions are crystalline and amorphous lamella, consisting mainly of amylopectin double helices, while the amorphous regions are disordered and extended side chains of amylopectin and interspersed amylose chains (Wang and Copeland, 2013). Various modes of granular erosion were therefore observed for samples incubated with the supernatant from ER T12 or parental ER supplemented with GSHE. This finding indicates that the amylases in these samples have the ability to attack cereal starch granules in a number of different ways. This gives further insight into the mechanism of increased starch hydrolysis by the novel amylase combination produced by ER T12.

3.5 Fermentations

Ideally, biofuel substrates would be fermented via CBP without the need for any exogenous enzyme addition (Van Zyl et al., 2012). Although this has previously been reported with broken rice as substrate (Favaro et al., 2017), the ethanol yields (about 70 g/L from of 20% dw/v broken rice) must be improved before the process can be considered for commercial implementation. The ER T12 and M2n T1 industrial strains have proven their amylolytic and fermentative capabilities using lab grade corn starch as substrate (Cripwell et al., 2019b) and are therefore good contenders for evaluation on broken rice.

Ethanol productivity by recombinant industrial amylolytic strains, in particular ER T12 and M2n T1, was evaluated through the saccharification and fermentation of 20% dw/v broken rice in different fermentation configurations. Firstly, fermentation with SSF (parental strains with 100% GSHE supplementation) was compared with supplemented CBP (recombinant strains ER

T12 or M2n T1 with the addition of 10% GSHE), and conventional CBP (only the recombinants ER T12 or M2n T1). Subsequently, the ER T12 strain was tested under more industrially applicable conditions by replacing media with water and conducting conventional CBP fermentations at 30 and 37°C.

3.5.1 SSF versus supplemented CBP fermentations

The ER and M2n parental strains supplemented with 100% GSHE in a SSF configuration only reached 75.02 and 79.45 g/L ethanol after 96 h, respectively, corresponding to estimated carbon conversions of 78 and 81% and $Y_{E/S}$ values of 78 and 81% (Table 2 and Fig. 3). However, when *S. cerevisiae* ER T12 was supplemented with 10% GSHE, it displayed an estimated carbon conversion of 100% and a 100% theoretical ethanol yield ($Y_{E/S}$) after 96 h with an ethanol productivity rate of 1.07 g/L/h (Table 2 and Fig. 3). Similarly, the M2n T1 strain supplemented with 10% GSHE displayed a 99% estimated carbon conversion, 99% $Y_{E/S}$ and an ethanol productivity rate of 1.04 g/L/h.

Fig. 3

After 168 h, near identical ethanol levels were obtained for the supplemented ER T12 and M2n T1 strains, i.e. 99.49 and 99.59 g/L (Table 2). The two SSF fermentations with the parental strains still lagged behind, with 86.81 and 90.40 g/L for ER and M2n, respectively. The two (supplemented) recombinant strains thus reached higher ethanol concentrations than their respective parental strains, even though the latter had a 10-fold GSHE load (100 versus 10%). The higher final ethanol concentrations achieved by the amylolytic yeast strains demonstrated the value of continuous amylase production in industrial fermentations. Glycerol was detected in

366 all the fermentation configurations, with ER T12 (10% GSHE) producing the highest
367 concentration after 168 h (3.93 g/L - Supplementary material). However, the accumulation of
368 glycerol was not considered a significant loss of carbon for ethanol production (Huang et al.,
369 2015). With respect to the recent trend in engineering industrial yeast strains for reduced glycerol
370 production (e.g. TransFerm® Yield+ from Lallemand,
371 www.lallemandbds.com/products/transferm-yield), it is significant to note that ER T12 produced
372 minor amounts of glycerol whilst maintaining high ethanol titers. Other fermentation products
373 (e.g. glucose, maltose and acetic acid) were also detected at low concentrations (Supplementary
374 material), thus further indicating a major flux of carbon towards ethanol.

375 **Table 2**

376

377 The rate at which ethanol was produced by the yeast strains in different fermentation
378 configurations is also noteworthy (Fig.3). After 24 h, *S. cerevisiae* ER T12 supplemented with
379 10% GSHE reached similar ethanol concentrations than the ER parental strain supplemented
380 with 100% GSHE (33.40 vs 29.55 g/L). Although supplemented M2n T1 produced lower ethanol
381 levels than the M2n parental strain (23.91 vs 31.94 g/L) after 24 h, similar concentrations were
382 achieved after 48 h. The superior performance by ER T12 can be attributed to its higher
383 volumetric activity and enzyme production (Fig. 1A), which results in quicker hydrolysis of
384 broken rice and thus increased ethanol production. Notably, the ER T12 strain supplemented
385 with 10% GSHE produced significantly higher ethanol titers from 48 h onwards when compared
386 to its parental strain supplemented with 100% GSHE. The fermentation with ER T12
387 supplemented with 10% GSHE was completed after 96 h, when the estimated carbon conversion
388 and $Y_{E/S}$ both reached 100% (Table 2).

389 In a recent study, Cripwell et al (2019b) compared the ER T12 and M2n T1 strains to SSF
390 fermentations conducted with the corresponding parental strains on raw corn starch. When a 10%
391 GSHE dosage was used in combination with the recombinant strains, ethanol levels were similar
392 to those obtained by the parental strains under SSF conditions after 48 h fermentation. The
393 results from the current study on broken rice followed a similar trend, however higher ethanol
394 yields were now achieved by the recombinant strains after only 48 h (Fig. 3). Thus, the
395 recombinant strains outperformed their parental counterparts on untreated broken rice with 10-
396 time less GSHE cocktail added to the fermentation, with the best performing strain, ER T12,
397 completing the fermentation within 96 h.
398
399 *3.5.2 Conventional CBP fermentations with ER T12 and M2n T1*
400 As reported in the previous section, both the ER T12 and M2n T1 recombinant strains reached
401 theoretical maximum yields when supplemented with 10% GSHE. We thus sought to evaluate
402 the performance of these strains in conventional CBP fermentations without any GSHE
403 supplementation. The ER T12 strain showed substantially higher ethanol concentrations (25.70
404 g/L) than the M2n T1 counterpart (14.14 g/L) after 24 h (Fig. 3). This trend continued up to 120
405 h, after which the deficit decreased and ER T12 and M2n T1 yielded similar ethanol levels at 168
406 h, i.e. 100.83 and 100.23 g/L, respectively. After 96 h of conventional CBP fermentation, ER
407 T12 produced 93% of the theoretical ethanol yield, while M2n T1 reached 79% (Table 2). The
408 ER T12 strain also displayed a higher ethanol productivity throughout the conventional CBP
409 fermentation compared to SSF with the parental ER strain and 100% GSHE loading. Both
410 recombinant strains reached estimated carbon conversions and $Y_{E/S}$ values of 100% at the end of
411 the fermentation (Table 2), confirming that the recombinant ER T12 and M2n T1 strains could

412 fully utilise the broken rice's starch without any pre-treatment or the addition of exogenous
413 GSHE cocktails.

414 In a previous study using the M2n[TLG1-SFA1] and MEL2[TLG1-SFA1] amylolytic yeast
415 strains, the highest ethanol yields reported from raw broken rice (20% w/v substrate loading)
416 were 74.54 and 67.97 g/L, respectively, after 144 h of fermentation (Favaro et al., 2017). Ethanol
417 concentrations recorded in the current study demonstrated that the ER T12 and M2n T1 strains
418 are superior for the CBP of broken rice. Specifically, the ER T12 strain reached higher ethanol
419 concentrations within 72 h (85.02 g/L) than reported by Favaro et al (2017) for M2n[TLG1-
420 SFA1] after 144 h (74.54 g/L). The ER T12 and M2n T1 strains also displayed higher theoretical
421 ethanol yields (based on total available glucose equivalents) and achieved complete utilization of
422 the substrate (100% estimated carbon conversion). This improved ethanol yield and productivity
423 was observed even though a significantly lower inoculum size (corresponding to nearly 3.5 g/L
424 wet cell weight) was used in the current study, compared to 50 g/L wet cell weight used
425 previously (Favaro et al., 2017). Increasing the size of yeast inoculum has been shown to
426 increase ethanol and glycerol yields, while simultaneously decreasing the fermentation time due
427 to a shorter lag phase during yeast growth (Ding et al., 2009). Therefore, it is possible that an
428 increase in ER T12 inoculum size may further enhance ethanol productivity, thereby decreasing
429 the fermentation period needed for complete conversion of broken rice via CBP.

430

431 *3.5.3 Comparing GSHE supplemented CBP with conventional CBP*

432 The ER T12 strain also produced significantly higher ethanol concentrations (70.52 vs 22.63
433 g/L) after 72 h fermentation on raw corn starch when supplemented with a 10% GSHE loading
434 (Cripwell et al., 2019b). The addition of 10% GSHE did not substantially increase the ethanol

concentrations from broken rice in the current study for the ER T12 strain, which indicated that complete mitigation (100% reduction) of exogenous enzyme loading can be achieved (Fig. 3). However, a significant difference in ethanol concentrations were observed between conventional CBP and GSHE supplemented CBP fermentations with the M2n T1 strain (Fig. 3). After 72 h, 10% GSHE supplemented CBP with M2n T1 produced 17.97 g/L more ethanol than when the GSHE cocktail was omitted, a trend observed in a previous study (Cripwell et al., 2019b).

Therefore, the ER T12 strain produced sufficient levels of starch degrading enzymes to render the addition of 10% GSHE redundant and has the qualities to be used as an amylolytic CBP yeast for ethanol production from raw broken rice. This could have large economic implications for starch-to-ethanol refineries by eliminating substrate pre-treatment, as well as liquefaction and saccharification steps from the current process. The ER T12 strain was therefore further evaluated in subsequent CBP fermentation studies to assess its performance under more industrially relevant conditions.

3.5.4 Evaluating ER T12 under more industrially relevant fermentation conditions

The use of expensive media components is undesirable in industrial starch-to-ethanol fermentations due to the large reactor volumes and financial implications (Bothast and Schlicher, 2005). However, proteases or a nitrogen source, like urea and corn steep liquor, are often added to support and enhance yeast growth in industrial processes (Bothast and Schlicher, 2005). The ability of *S. cerevisiae* ER T12 to process broken rice into ethanol without added proteases, nitrogen or other nutrients was evaluated at 30°C using sterilised RO water as a replacement for concentrated YPD broth. Although the ER T12 strain produced less ethanol than with concentrated YPD between 48 h and 72 h (Fig. 4A), the ethanol concentration reached 96.66 g/L

458 with RO water after 168 h, in comparison to 98.03 g/L for concentrated YPD broth. At 168 h,
459 98% of the carbon was converted to products and an ethanol yield of 98% was obtained, which
460 was only 1% lower than when concentrated YPD had been used and is not considered a
461 significant difference (p = 0.12).

462 **Fig. 4**

463

464 Broken rice contained significant amounts of protein (8.47%, Supplementary material) that
465 could be utilised by the yeast as a source of nitrogen. It has been suggested that *S. cerevisiae* has
466 a preference to assimilate peptides as a nitrogen source in the presence of ammonia and free
467 amino acids (Kevvai et al., 2016). This could explain how fermentations using RO water
468 progressed at a rate similar to fermentations containing concentrated YPD (Fig. 4A). From these
469 results there is evidence for excluding the addition of external nutrients (specifically nitrogen) at
470 the start of industrial fermentations, when using substrates such as broken rice in combination
471 with highly efficient amylolytic yeast strains. This would simplify the fermentation setup and
472 further reduce costs associated with the process by possibly eliminating nitrogen and/or protease
473 addition.

474 A higher fermentation temperature is a desired parameter in industrial starch-to-ethanol
475 processes (Abdel-Banat et al., 2010; Walker and Walker, 2018) as it increases the hydrolytic
476 activity of the amylase enzymes (and subsequently starch hydrolysis) and decreases costs related
477 to temperature control/changes (Görgens et al., 2015). When the *S. cerevisiae* ER T12 strain was
478 used for the CBP of broken rice at 37°C, it resulted in an initial increase in ethanol production
479 within the first 48 h, most likely due to the greater activity of amylases at the higher temperature
480 (Fig. 4B). However, an incomplete fermentation was reached after 72 h and the ethanol

concentrations plateaued at ~69.40 g/L. This is in agreement with fermentation results from a previous study on raw corn starch, which highlighted that ER T12's fermenting ability was compromised at 37°C (Cripwell et al., 2019b). Furthermore, the high residual glucose concentrations (>40 g/L, Fig 4D) is also an indicator of an incomplete fermentation, while at the same time demonstrating the superior hydrolytic ability of the recombinant enzyme combination produced by ER T12. The observed arrest in fermentation is probably a result of physiological changes to the yeast, which is thought to be associated with membrane composition changes in response to temperature stress; this was previously described as a strain-specific trait in *S. cerevisiae* (Henderson et al., 2013). However, additional studies are required to confirm this hypothesis for both the *S. cerevisiae* ER and ER T12 strains. A further decrease in final ethanol concentrations was observed when YPD was replaced with RO water, with an ethanol production that remained at approximately 50 g/L after 72 h. Moreover, the addition of 16 mM urea as extra nitrogen source did not enable the *S. cerevisiae* ER T12 strain to recover from any of the additional stresses caused by a higher fermentation temperature and ethanol concentrations were lower than those obtained when YPD broth was used. This suggested that the incomplete fermentation at 37°C was mainly due to temperature stress and not nitrogen limitation.

The ER parental strain is considered as a relatively thermo-tolerant yeast strain and is widely used in industry for various fermentative purposes. However, results reported here, together with other findings (Costa et al., 2017; Cripwell et al., 2019b; Gronchi et al., 2019), suggested that thermo-tolerance still remains a major challenge in the development of improved industrial yeast strains.

4. Conclusions

The utilization of alternative feedstocks in CBP fermentations using amylolytic yeast strains can enhance economical ethanol production on an industrial scale. In this study, crude enzymes from recombinant yeast strains showed saccharification yields comparable to a commercial GSHE cocktail using untreated broken rice. During fermentation experiments the addition of exogenous GSHE cocktail did not improve ethanol production significantly. Compared to previous raw starch CBP reports, the industrial ER T12 strain produced higher ethanol concentrations at a faster rate from raw broken rice. The strain can thus be regarded as an ideal CBP yeast for commercial ethanol production from starchy substrates.

Acknowledgements

The authors would like to thank Prof Lydia Joubert (CAF/ Stellenbosch University) for assistance with SEM imaging, as well as Mrs Lisa Warburg (Stellenbosch University) for assistance with HPLC analysis.

Competing interests

The authors declare that they have no competing interests.

Funding

This work was supported by the National Research Foundation (NRF) for financial support to grant holders and through the bilateral joint research project between Italy and South Africa [grant 113134 and ZA18MO04, respectively].

Supplementary material

E-Supplementary data associated with this article can be found in the online version.

References

1. Abdel-Banat, B.M.A., Hoshida, H., Ano, A., Nonklang, S., Akada, R., 2010. High-temperature fermentation: How can processes for ethanol production at high temperatures become superior to the traditional process using mesophilic yeast? Appl. Microbiol. Biotechnol. 85, 861-867.
2. AOAC, 2000. Official Methods of Analysis of AOAC International. Assoc. Off. Anal. Chem. Int.
3. Atitallah, I. B., Antonopoulou, G., Ntaikou, I., Alexandropoulou, M., Nasri, M., Mechichi, T., Lyberatos, G., 2019. On the evaluation of different saccharification schemes for enhanced bioethanol production from potato peels waste via a newly isolated yeast strain of *Wickerhamomyces anomalus*. Bioresour. Technol. 289, 121614.
4. Bertoft, E., 2017. Understanding starch structure: Recent progress. Agronomy. 7, 56.
5. Blazek, J., Gilbert, E.P., 2010. Effect of enzymatic hydrolysis on native starch granule structure. Biomacromolecules. 11, 3275-3289.
6. Bothast, R.J., Schlicher, M.A., 2005. Biotechnological processes for conversion of corn into ethanol. Appl. Microbiol. Biotechnol. 67, 19-25.
7. Chandel, A. K., Garlapati, V. K., Singh, A. K., Antunes, F. A. F., da Silva, S. S., 2018. The path forward for lignocellulose biorefineries: bottlenecks, solutions, and perspective on commercialization. Bioresour. Technol. 264, 370-381.

8. Chu-Ky, S., Pham, T.H., Bui, K.L.T., Nguyen, T.T., Pham, K.D., Nguyen, H.D.T., Luong, H.N., Tu, V.P., Nguyen, T.H., Ho, P.H., Le, T.M., 2016. Simultaneous liquefaction, saccharification and fermentation at very high gravity of rice at pilot scale for potable ethanol production and distillers dried grains composition. Food Bioprod. Process. 98, 79-85.
9. Cripwell, R., Favaro, L., Rose, S.H., Basaglia, M., Cagnin, L., Casella, S., van Zyl, W.H., 2015. Utilisation of wheat bran as a substrate for bioethanol production using recombinant cellulases and amylolytic yeast. Appl. Energy 160, 610-617.
10. Cripwell, R.A., Rose, S.H., Viljoen-Bloom, M., van Zyl, W.H., 2019a. Improved raw starch amylase production by *Saccharomyces cerevisiae* using codon optimisation strategies. FEMS Yeast Res. 19, 1-14.
11. Cripwell, R.A., Rose, S.H., Favaro, L., van Zyl, W.H., 2019b. Construction of industrial *Saccharomyces cerevisiae* strains for the efficient consolidated bioprocessing of raw starch. Biotechnol. Biofuels 12, 201.
12. Costa, C. E., Romaní, A., Cunha, J. T., Johansson, B., Domingues, L., 2017. Integrated approach for selecting efficient *Saccharomyces cerevisiae* for industrial lignocellulosic fermentations: importance of yeast chassis linked to process conditions. Bioresour. Technol. 227, 24-34.
13. Devantier, R., Pedersen, S., Olsson, L., 2005. Characterization of very high gravity ethanol fermentation of corn mash. Effect of glucoamylase dosage, pre-saccharification and yeast strain. Appl. Microbiol. Biotechnol. 68, 622-629.
14. Dhital, S., Gidley, M.J., Warren, F.J., 2015. Inhibition of α-amylase activity by cellulose: Kinetic analysis and nutritional implications. Carbohydr. Polym. 123, 305-312.

15. Ding, M.Z., Tian, H.C., Cheng, J.S., Yuan, Y.J., 2009. Inoculum size-dependent interactive regulation of metabolism and stress response of *Saccharomyces cerevisiae* revealed by comparative metabolomics. J. Biotechnol. 144, 279-286.

16. DuPont, 2012. Granular starch hydrolyzing enzyme for ethanol production. 2-3.

17. Favaro, L., Basaglia, M., Saayman, M., Rose, S., van Zyl, W.H., Casella, S., 2010. Engineering amylolytic yeasts for industrial bioethanol production. Chem. Eng. Trans. 20,97-102.

18. Favaro, L., Basaglia, M., Casella, S., 2012a. Processing wheat bran into ethanol using mild treatments and highly fermentative yeasts. Biomass Bioenergy 46, 605-617.

19. Favaro, L., Jooste, T., Basaglia, M., Rose, S.H., Saayman, M., Görgens, J.F., Casella, S., van Zyl, W.H., 2012b. Codon-optimized glucoamylase sGAI of *Aspergillus awamori* improves starch utilization in an industrial yeast. Appl. Microbiol. Biotechnol. 95, 957-968.

20. Favaro, L., Jooste, T., Basaglia, M., Rose, S.H., Saayman, M., Görgens, J.F., Casella, S., van Zyl, W.H., 2013. Designing industrial yeasts for the consolidated bioprocessing of starchy biomass to ethanol. Bioengineered 4,97-102.

21. Favaro, L., Viktor, M.J., Rose, S.H., Viljoen-Bloom, M., van Zyl, W.H., Basaglia, M., Cagnin, L., Casella, S., 2015. Consolidated bioprocessing of starchy substrates into ethanol by industrial *Saccharomyces cerevisiae* strains secreting fungal amylases. Biotechnol. Bioeng. 112, 1751-1760.

22. Favaro, L., Cagnin, L., Basaglia, M., Pizzocchero, V., van Zyl, W.H., Casella, S., 2017. Production of bioethanol from multiple waste streams of rice milling. Bioresour. Technol. 244, 151-159.

593 23. Favaro L., Jansen T., van Zyl W.H., 2019. Exploring industrial and natural *Saccharomyces*
594 *cerevisiae* strains for the bio-based economy from biomass: the case of bioethanol. Crit. Rev.
595 Biotechnol. 39, 800-816.
596 24. Gohel, V., Duan, G., 2012. No-Cook process for ethanol production using indian broken rice
597 and pearl millet. Int. J. Microbiol. doi:10.1155/2012/680232.
598 25. Görgens, J.F., Bressler, D.C., van Rensburg, E., 2015. Engineering *Saccharomyces*
599 *cerevisiae* for direct conversion of raw, uncooked or granular starch to ethanol. Crit. Rev.
600 Biotechnol. 35, 369-391.
601 26. Gronchi, N., Favaro, L., Cagnin, L., Brojanigo, S., Pizzocchero, V., Basaglia, M., Casella, S.,
602 2019. Novel yeast strains for the efficient saccharification and fermentation of starchy by-
603 products to bioethanol. Energies. 12, 714.
604 27. Henderson, C.M., Zeno, W.F., Lerno, L.A., Longo, M.L., Block, D.E., 2013. Fermentation
605 temperature modulates phosphatidylethanolamine and phosphatidylinositol levels in the cell
606 membrane of *Saccharomyces cerevisiae*. Appl. Environ. Microbiol. 79, 5345–5356.
607 28. Huang, H., Qureshi, N., Chen, M.H., Liu, W., Singh, V., 2015. Ethanol production from food
608 waste at high solids content with vacuum recovery technology. J. Agric. Food Chem. 63,
609 2760-2766.
610 29. Kevvai, K., Kütt, M.L., Nisamedtinov, I., Paalme, T., 2016. Simultaneous utilization of
611 ammonia, free amino acids and peptides during fermentative growth of *Saccharomyces*
612 *cerevisiae*. J. Inst. Brew. 122, 110-115.
613 30. Liao, B., Hill, G.A., Roesler, W.J., 2012. Stable expression of barley α-amylase in *S.*
614 *cerevisiae* for conversion of starch into bioethanol. Biochem. Eng. J, 64, 8-16.

31. Mathew, A.S., Wang, J., Luo, J., Yau, S.T., 2015. Enhanced ethanol production via electrostatically accelerated fermentation of glucose using *Saccharomyces cerevisiae*. Sci. Rep. 5, 1-6.

32. Matsushima, R., Maekawa, M., Sakamoto, W., 2015. Geometrical formation of compound starch grains in rice implements Voronoi diagram. Plant Cell Physiol. 56, 2150-2157.

33. Meredith, J., 2003. Understanding energy use and energy users in contemporary ethanol plants, fourth ed, The alcohol textbook. Nottingham, UK.

34. Miller, G.L., 1959. Use of dinitrosalicylic acid reagent for determination of reducing sugar. Anal. Chem. 31, 426-428.

35. Niphadkar, S., Bagade, P., Ahmed, S., 2018. Bioethanol production: insight into past, present and future perspectives. Biofuels. 9, 229-238.

36. Nizami, A. S., Rehan, M., Waqas, M., Naqvi, M., Ouda, O. K. M., Shahzad, K., Miandad, R., Khan, M.Z., Syamsiro, M., Ismail, I.M.I., Pant, D., 2017. Waste biorefineries: enabling circular economies in developing countries. Bioresour. Technol. 241, 1101-1117.

37. Ntaikou, I., Menis, N., Alexandropoulou, M., Antonopoulou, G., Lyberatos, G., 2018. Valorization of kitchen biowaste for ethanol production via simultaneous saccharification and fermentation using co-cultures of the yeasts *Saccharomyces cerevisiae* and *Pichia stipitis*. Bioresour. Technol. 263, 75-83.

38. Renewable Fuels Association, 2017. Pocket guide to ethanol.

39. Sakwa, L., Cripwell, R.A., Rose, S.H., Viljoen-Bloom, M., 2018. Consolidated bioprocessing of raw starch with *Saccharomyces cerevisiae* strains expressing fungal alpha-amylase and glucoamylase combinations. FEMS Yeast Res. 18, foy085.

637 40. Sindhu, R., Binod, P., Pandey, A., 2016. Biological pretreatment of lignocellulosic biomass–
638 an overview. Bioresour. Technol. 199, 76-82.
639 41. Sujka, M., Jamroz, J., 2007. Starch granule porosity and its changes by means of amylolysis.
640 Int. agrophysics 21, 107-113.
641 42. Theander, O., Aman, P., Westerlund, E., Andersson, R., Pettersson, D., 1995. Total dietary
642 fiber determined as neutral sugar residues, uronic acid residues, and Klason lignin (the
643 Uppsala method): collaborative study. J. AOAC Int. 78, 1030-1044.
644 43. Van Zyl, W.H., Bloom, M., Viktor, M.J., 2012. Engineering yeasts for raw starch conversion.
645 Appl. Microbiol. Biotechnol. 95, 1377-1388.
646 44. Viktor, M.J., Rose, S.H., van Zyl, W.H., Viljoen-Bloom, M., 2013. Raw starch conversion by
647 *Saccharomyces cerevisiae* expressing *Aspergillus tubingensis* amylases. Biotechnol.
648 Biofuels. 6, 167.
649 45. Walker, G.M., Walker, R.S.K., 2018. Enhancing yeast alcoholic fermentations. Adv. Appl.
650 Microbiol. 105, 87-129.
651 46. Wang, J.P., Zeng, A.W., Liu, Z., Yuan, X.G., 2006. Kinetics of glucoamylase hydrolysis of
652 corn starch. J. Chem. Technol. Biotechnol. 81, 727-729.
653 47. Wang, S., Copeland, L., 2013. Molecular disassembly of starch granules during
654 gelatinization and its effect on starch digestibility: A review. Food Funct. 4, 1564-1580.
655 48. Yamada, R., Tanaka, T., Ogino, C., Fukuda, H., Kondo, A., 2010. Novel strategy for yeast
656 construction using δ-integration and cell fusion to efficiently produce ethanol from raw
657 starch. Appl. Microbiol. Biotechnol. 85, 1491-1498.
658 49. Yu, J., Xu, Z., Liu, L., Chen, S., Wang, S., Jin, M., 2019. Process integration for ethanol
659 production from corn and corn stover as mixed substrates. Bioresour. Technol. 279, 10-16.

50. Zabed, H., Sahu, J.N., Suely, A., Boyce, A.N., Faruq, G., 2017. Bioethanol production from renewable sources: Current perspectives and technological progress. Renew. Sustain. Energy Rev. 71, 475-501.

683 **Figures captions**

684

685 **Fig 1.** A) Volumetric enzyme activity (solid lines) and correlating protein concentration (dashed
686 lines) profiles over time for the *S. cerevisiae* ER T12 (◆) and M2n T1 (■) strains. B) Total
687 reducing sugar ends and (C) glucose yields by supernatants of the amylolytic *S. cerevisiae* ER
688 T12 (striped bars) and M2n T1 (dotted bars) strains after hydrolysis of 2% dw/v broken rice, at
689 30°C. Error bars represent standard deviation from the mean of three replicates.

690

691 **Fig 2.** A) Glucose and (B) maltose concentrations detected during the scaled-up hydrolysis of
692 20% dw/v broken rice at 30°C. Data for (◆) *S. cerevisiae* ER T12 supernatant as well as parental
693 ER supernatant supplemented with 200% (●), 100% (▲) and 50% (■) GSHE loadings is
694 reported. (C) Degree of saccharification (DS) of 20% dw/v broken rice by *S. cerevisiae* ER T12
695 supernatant (with no addition of enzymes) and ER supernatant supplemented with 200, 100 and
696 50% GSHE loadings, respectively. Error bars represent standard deviation from the mean of
697 three replicates.

698

699 **Fig 3.** Ethanol concentrations detected during SSF (dotted lines), supplemented CBP (dashed
700 lines) and conventional CBP (solid lines) fermentations of 20% dw/v broken rice at 32°C using
701 the S. *cerevisiae* ER T12 (◆), M2n T1 (■), ER (▲) and M2n (●) strains. Error bars represent
702 standard deviation from the mean of three replicates.

703

704 **Fig 4.** Ethanol (A and B) and glucose (C and D) concentrations for conventional CBP
705 fermentations with ER T12, conducted at 30°C (A and C) and 37°C (B and D) using YPD broth

(solid line), RO water (dashed line) or RO water with 16 mM urea (dotted line) and 20% dw/v broken rice as substrate. Error bars represent standard deviation from the mean of three replicates.

729

730 **Table 1.** Yeast strains used during this study.

***S. cerevisiae* strains**	**Genotype**	**Reference/Source**
Ethanol Red™ Version 1	*MAT*a/α prototroph	Fermentis, Lesaffre, France
M2n	*MAT*a/α prototroph	Favaro et al., 2015
ER T12	δ-integration of *ENO1$_P$-temG_Opt-ENO1$_T$*; *ENO1$_P$-temA_-ENO1$_T$*	Cripwell et al., 2019b
M2n T1	δ-integration of *ENO1$_P$-temG_Opt-ENO1$_T$*; *ENO1$_P$-temA_-ENO1$_T$*	Cripwell *et al*., 2019b

731

732

733 **Table 2.** Summary of fermentation results after 96 h and 168 h at 32°C using 20% dw/v broken
734 rice in YPD broth.

Strain (fermentation configuration)	Ethanol (g/L)	$Y_{E/S}$ [a] (%)	Q (g/L/h) [b]	Carbon conversion (mol C) [c]	
ER (SSF) [d]	75.02	78	0.81	78%	**96 h**
ER T12 (supplemented CBP) [e]	101.38	100	1.07	100%	
ER T12 (CBP)	93.48	93	0.97	95%	
M2n (SSF) [d]	79.45	81	0.85	81%	
M2n T1 (supplemented CBP) [e]	97.30	99	1.04	99%	
M2n T1 (CBP)	76.69	79	0.82	79%	
ER (SSF) [d]	86.81	89	0.54	89%	**168 h**
ER T12 (supplemented CBP) [e]	99.49	100	0.60	100%	
ER T12 (CBP)	100.83	100	0.60	100%	
M2n (SSF) [d]	90.40	92	0.55	92%	
M2n T1 (supplemented CBP) [e]	99.59	100	0.61	100%	
M2n T1 (CBP)	100.23	100	0.60	100%	

735 [a] YE/S represents percentage of the maximum theoretical ethanol yield as calculated from total available glucose
736 equivalents
737 [b] Q represents the ethanol productivity as the amount of ethanol produced per hour (g/L/h)
738 [c] Carbon conversion was calculated on a mol C basis considering all products detected through HPLC
739 [d] SSF of non-recombinant parental strains supplemented with 100% GSHE loading
740 [e] Supplemented CBP of recombinant strains supplemented with 10% GSHE loading
741
742
743

Fig. 1.

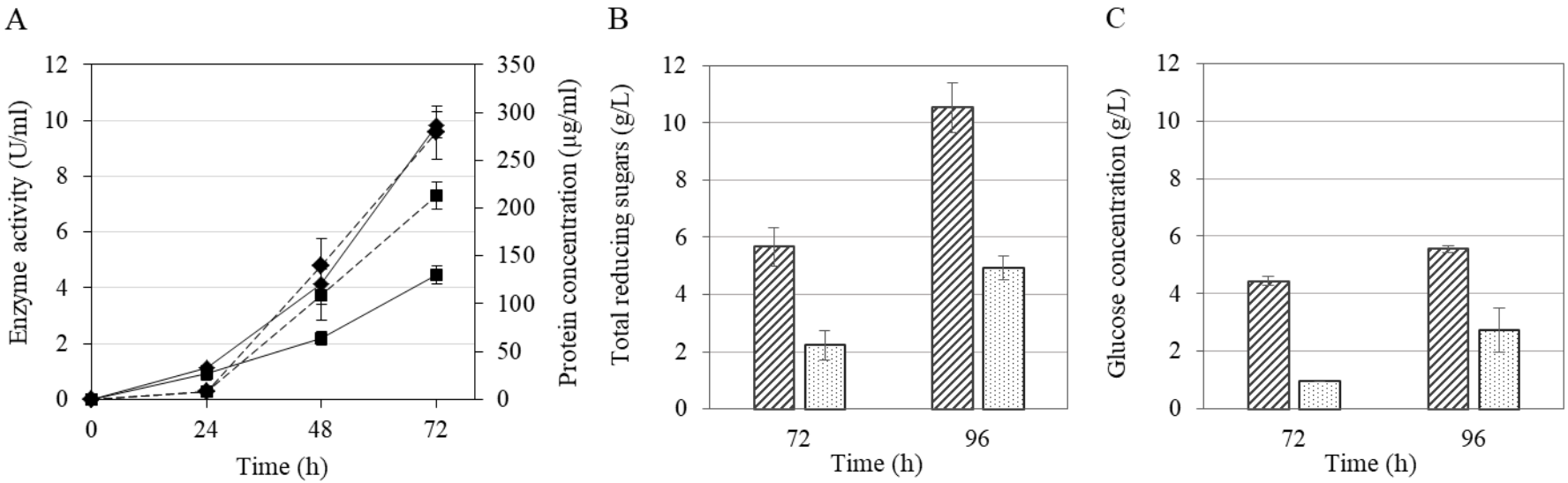
A
Enzyme activity (U/ml)
Protein concentration (µg/ml)
Time (h)
0
24
48
72
B
Total reducing sugars (g/L)
Time (h)
72
96
C
Glucose concentration (g/L)
Time (h)
72
96

Fig. 2.

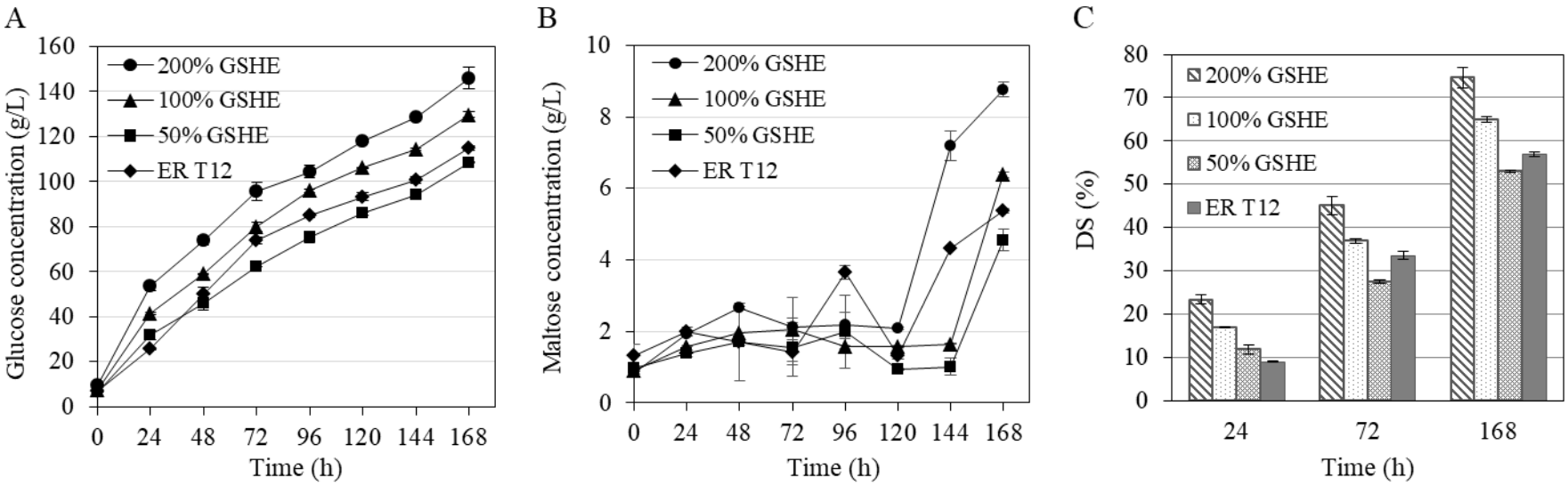
A
Glucose concentration (g/L)
160
140
120
100
80
60
40
20
0
200% GSHE
100% GSHE
50% GSHE
ER T12
0 24 48 72 96 120 144 168
Time (h)
B
Maltose concentration (g/L)
10
8
6
4
2
0
200% GSHE
100% GSHE
50% GSHE
ER T12
0 24 48 72 96 120 144 168
Time (h)
C
DS (%)
80
70
60
50
40
30
20
10
0
200% GSHE
100% GSHE
50% GSHE
ER T12
24 72 168
Time (h)

Fig. 3.

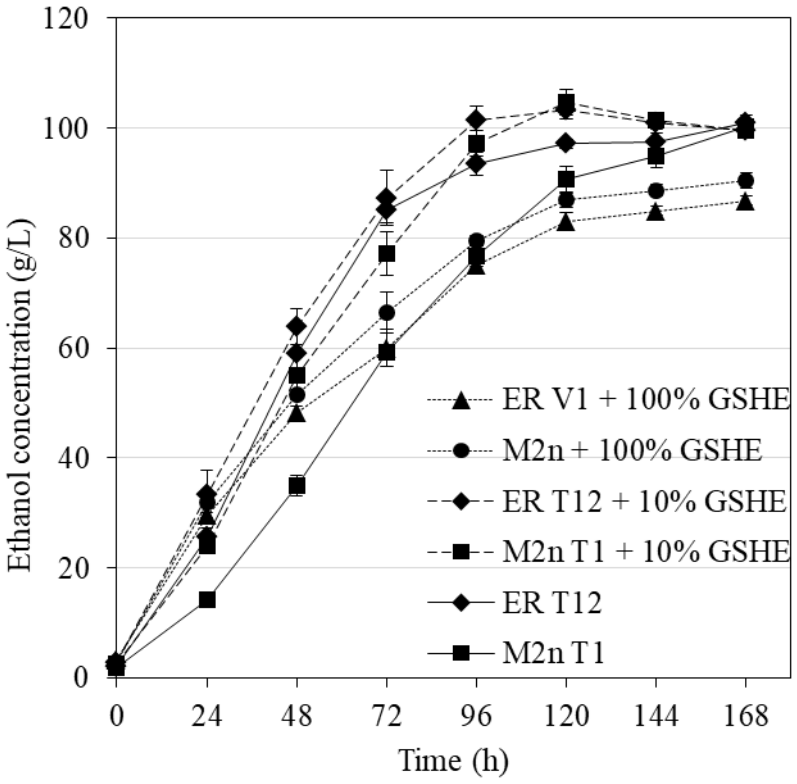
120
100
80
60
40
20
0
Ethanol concentration (g/L)
0
24
48
72
96
120
144
168
Time (h)
ER V1 + 100% GSHE
M2n + 100% GSHE
ER T12 + 10% GSHE
M2n T1 + 10% GSHE
ER T12
M2n T1

Fig. 4.

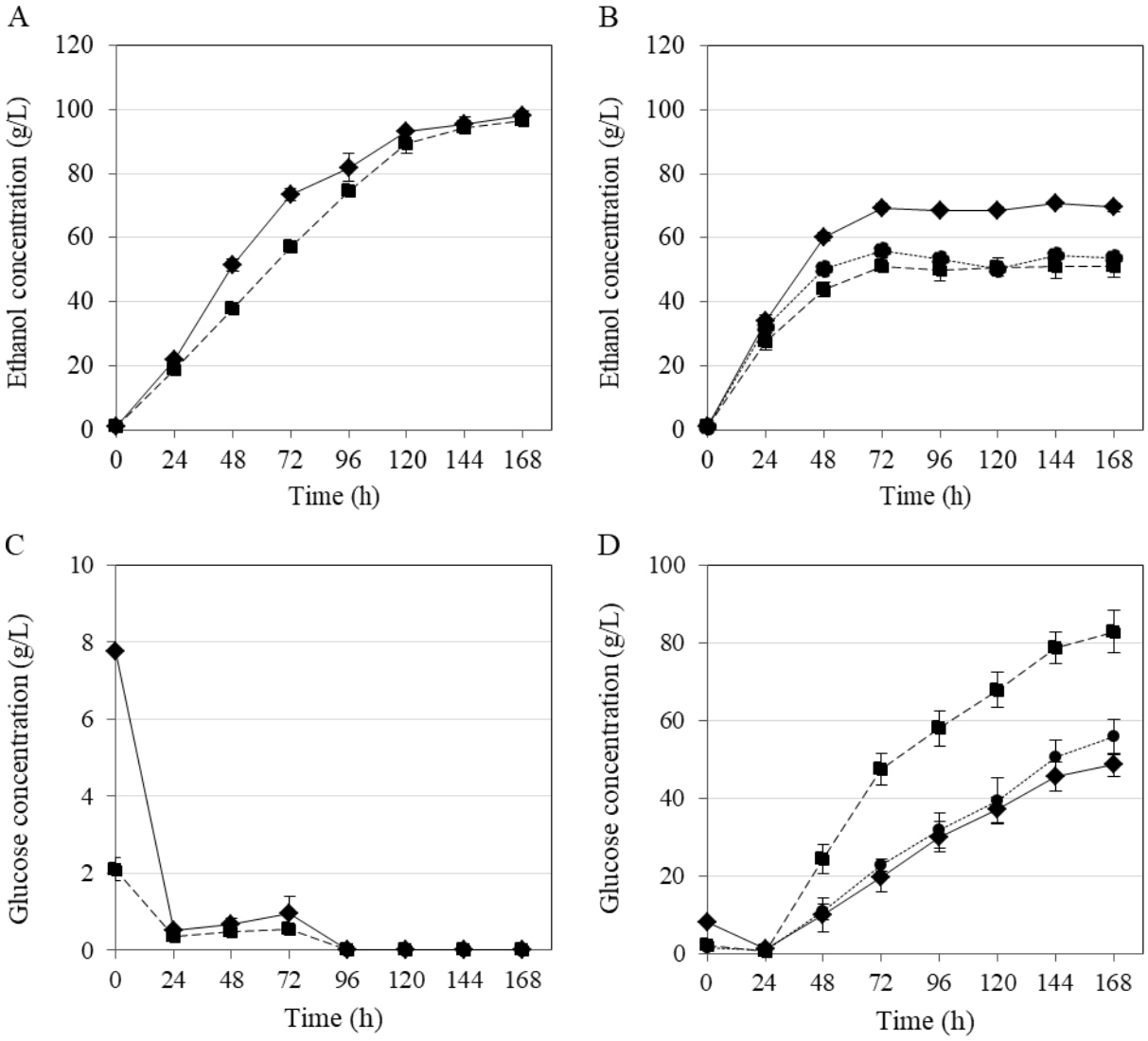
A
Ethanol concentration (g/L)
120
100
80
60
40
20
0
0 24 48 72 96 120 144 168
Time (h)
B
Ethanol concentration (g/L)
120
100
80
60
40
20
0
0 24 48 72 96 120 144 168
Time (h)
C
Glucose concentration (g/L)
10
8
6
4
2
0
0 24 48 72 96 120 144 168
Time (h)
D
Glucose concentration (g/L)
100
80
60
40
20
0
0 24 48 72 96 120 144 168
Time (h)